MRI-ULTRASOUND REGISTRATION FOR TARGETED PROSTATE BIOPSY

[1]*R. Narayanan,* [2]*J. Kurhanewicz,* [2]*K. Shinohara,* [3]*E. D. Crawford,* [4]*A. Simoneau, and* [1]*J. S. Suri*

[1]Eigen LLC, 13366 Grass Valley Ave., Grass Valley, CA, USA
[2]University of California, San Francisco, CA, USA
[3]University of Colorado, Denver, CO, USA
[4]University of California, Irvine, CA, USA

ABSTRACT

T2-weighted magnetic resonance images (MRI) imaging using an endorectal coil combined with a pelvic phased-array coil has been shown to provide high resolution images of the prostate. To integrate MRI analysis in standard prostate biopsy procedures, preoperative MRI must be accurately registered to 3-D transrectal ultrasound (TRUS) images. Shape changes due to patient motion, or drugs can induce further differences in glandular shape variation between preoperative MRI and 3-D TRUS during biopsy. In the proposed work, we model the deformation relating MRI and TRUS so as to enable analysis of MRI in conjunction with ultrasound (color blended or side-by-side) for planning of biopsy targets. Registration of MRI at various resolutions and endorectal balloon volumes and ultrasound volumes yielded average fiducial registration error of 3.06 mm using 6 and 12 bead phantoms.

Index Terms— prostate, cancer, biopsy, MRI, ultrasound

1. INTRODUCTION

Prostate cancer is the most common non-cutaneous cancer diagnosed amongst males in the United States [1]. Prostate specific antigen (PSA) measured via a blood test and digital rectal examination (DRE) are used to screen for prostate cancer, followed by a transrectal ultrasound (TRUS) guided biopsy to confirm. Commonly used TRUS images are not very effective in the detection of cancers. A study showed that 39% of cancers are isoechoic [2] making detection with TRUS difficult. Newer methods such as pulse inversion, color and power Doppler, elastography, contrast and harmonic imaging are starting to gain ground; it is still unclear how suspicious regions in enhanced TRUS images correlate with localized prostate cancers.

Magnetic resonance imaging (MRI) is being increasingly used in the assessment of prostate cancer. The excellent soft tissue contrast, and easily discernible zones within the prostate provides high sensitivity to cancers, which are typically seen as locations with decreased signal intensity relative to neighboring areas on T_2-weighted images. Magnetic resonance spectroscopy imaging (MRSI) provides a four dimensional image of the prostate, measuring the metabolite concentrations of choline, creatine, polyamine and citrate at every voxel on a phase encode spanning the prostate. A standardized scoring system was introduced by Jung *et al* [3] where four dimensional MRSI images were interpreted based on metabolic criteria, and each voxel was assigned a score of 1 (benign) to 5 (malignant). The high specificity of MRSI to metabolically identify cancer has improved the combined value of an MRI/MRSI exam. An additional advantage is that the two modalities are already coregistered, allowing MRSI to undergo the same transformation as MRI after registration. An in depth review of MRI/MRSI imaging for prostate cancer can be found in Kurhanewicz *et al* [4]. A more general review of current and emerging imaging techniques for prostate cancer is presented in Akin *et al* [5]. An immediate challenge in the effective use of MR data for biopsy lies in its registration to ultrasound that is used during biopsy.

Early on, a prototype of a prostate biopsy robot used inside a conventional MRI scanner was demonstrated [6]. However the use of such methods are uncommon due to the expense and relative complexity of such procedures. Other researchers have proposed using preoperative MRI registered to realtime ultrasound during the surgical procedure. A manual rigid registration was demonstrated by Kaplan *et al* [7] for prostate biopsy by finding the optimal transformation relating six fiducials manually identified on both preoperative MRI and realtime ultrasound. An improved system was proposed by Reynier *et al* [8] for brachytherapy where manually segmented point clouds from MRI and TRUS were used to either rigidly or elastically align MRI with TRUS. The advantage of this system was the ability to model potential nonlinear deformation between the two modalities due to deformation induced by the endorectal coil. However the contours needed to be manually delineated from both modalities. A real time fusion system [9] capable of rigid registration was proposed without manual delineation of boundaries. The authors used fiducials in the form of gold seeds on phantoms and estimated the rigid transformation based on correspondence. Manual registration on real subjects was carried out

by visualization of both 3-D MRI and 3-D ultrasound and adjusting rigid parameters. In later work by the same group [10], the researchers adopted a similar rigid registration strategy but additionally used the real time ultrasound image to compensate for any motion that may have caused the 2-D realtime image to go out of alignment within the preoperative 3-D ultrasound volume. These methods either used simplistic deformation models in the form of rigid or affine deformations, or required the manual delineation of boundaries which may be time consuming. The proposed work is motivated by the need to model accurately the deformation between the two modalities, while at the same time fast in order to be clinically useful. Speed optimizations are achieved via the use of a graphics processing unit (GPU). We present early results to show the clinical feasibility of such an approach needing further validation on real subjects.

We begin with a preoperatively acquired T_2-weighted MRI image followed by a full 3-D TRUS image acquisition just prior to biopsy. Both these volumes are subject to a semiautomatic segmentation [11] that involves the specification of four or more points along the gland boundary. The triangulated gland surfaces from both modalities are registered using an adaptive focus deformable model [12] following by elastically interpolating the entire MRI volume to align with TRUS. We demonstrate a preliminary experiment on a multimodality phantom from CIRS (Norfolk, Virginia) with six embedded glass beads. The ultrasound volume was scanned using an end-fired TRUS probe and the T_2-weighted axial fast spin echo MRI volumes were acquired on a 3T GE MRI with and without endorectal coil. Both surface registration and the elastic interpolation methods were implemented in Artemis^{TM}(Eigen Inc., Grass Valley, California) that used computed unified device architecture (CUDA) supported graphics processing unit (GPU) to achieve less than 13 seconds computation time, and approximately 30 seconds including the time taken to semiautomatically segment both MRI and ultrasound volumes.

As acknowledged by Xu [10] it is possible that the prostate may move after the acquisition of the 3-D volume. As a result there is a need to constantly update the position of the realtime slice with reference to the 3-D volume. They used multiple frames using a sum-of-squared distance cost function to orient the 3-D volume with respect to current orientation. Shen *et al* [13] proposed using crosscorrelation to register the realtime ultrasound slice to the 3-D volume on a GPU achieving a speed of 0.46 seconds working on 2-D images containing 91,000 pixels. An improvement to 0.19 seconds was achieved after downsampling the data by two levels. On registration, the operator can view both MRI and ultrasound volumes in multiple ways to target sites for biopsy; a toggle function allows the user to view one or the other for the same slice section being displayed. Varying degrees of blending can also be visualized. A third functionality allows the user to view both volumes simultaneously being sliced or reoriented.

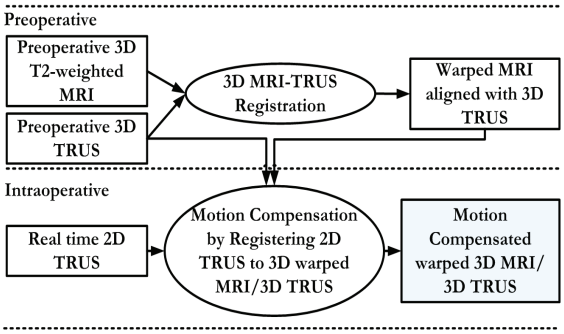

Fig. 1. MRI-TRUS fusion system with motion compensation.

2. METHOD

Image fusion in Artemis^{TM}is part of the planning process during the biopsy procedure. Figure 1 shows a fusion system used for biopsy. The procedure begins with the acquisition of an MRI T_2-weighted axial fast spin echo image few days or weeks prior to biopsy. A 3-D TRUS is acquired just prior to biopsy by reconstructing sweeps of 2-D to 3-D. The two volumes are registered so as to align the MRI volume with the 3-D TRUS volume. Finally during biopsy, as the operator visualizes the realtime ultrasound volume on screen, and motion compensation (MC) to compensate for any movement of the prostate after the acquisition of the 3-D volume runs automatically every few hundred milliseconds. Finally the original 3-D TRUS volume and warped MRI volume are both readjusted so as to correspond with the real time 2D ultrasound image.

3. IMPLEMENTATION

Intensity based nonrigid registration of 3-D multi-modality images is in general computationally intensive. Registration times typically vary between a few minutes to hours depending on the deformation model, degrees of freedom used, and image sizes. This can be especially challenging in a clinical situation where fast registration times can help speed up workflow, reduce patient anxiety and reduce motion related misalignments. In the proposed method we registered the TRUS and MRI surface followed by elastically interpolating the MRI volume to align it with that of TRUS. Registration was carried out in four steps:

1. Segmentation of MRI and Ultrasound Volumes
2. Global surface alignment
3. Deformable surface registration
4. Elastically warping MRI to TRUS

Segmentation of MRI and ultrasound volumes is accomplished using a discrete dynamic contour [11] via the initial-

ization of 4 or more points on the boundary of the prostate. In the second step, the MRI surface (S_{MRI}) is iteratively globally aligned to the TRUS surface (S_{TRUS}) using an extended weighted procrustes analysis [14]. Vertices that are not in alignment with corresponding vertices are weighted higher in estimating the global rotation and translation parameters. The weights were set directly equal to the distance of all vertices from S_{MRI} to S_{TRUS}. The result of this alignment was a rigidly transformed surface, S'_{MRI}. After global alignment the tentative surface S'_{MRI} and the TRUS surface S_{TRUS} are nonlinearly registered using an adaptive focus deformable model (AFDM) [12]. Finally the MRI volume is elastically warped [15] using these boundary conditions and interpolated to arrive at the resulting warped MRI volume in alignment with the 3-D TRUS image. Figure 2(a) shows misalignment

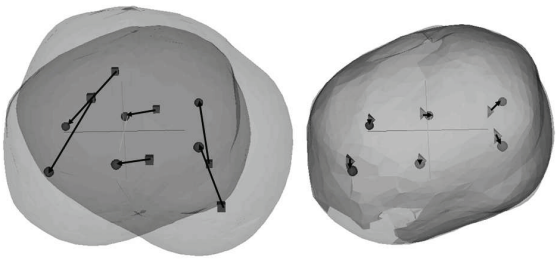

(a) Before Registration (b) After Registration

Fig. 2. (a) Prostate surface from ultrasound and MRI originally misaligned showing corresponding beads as cubes and spheres respectively.(b) Warped ultrasound surface and surface from MRI overlaid showing corresponding beads as cones and spheres. Arrows show original and final correspondence between bead positions.

of S_{TRUS} and S_{MRI} before registration. Also seen are corresponding beads in both modalities (spheres on MRI and cubes in TRUS). Figure 2(b) shows improved bead correspondence after registration. Also seen are the warped TRUS surface overlaid on the surface from MRI after AFDM. Figure 3 shows registered results from real data, where the top two rows shows various degrees of blending between TRUS and MRI. Both MRI and TRUS can also be visualized blended as shown or side-by-side to enable more intuitive selection of target sites, i.e. top left and bottom right viewed next to each other.

4. RESULTS

In order to validate our registration, experiments were carried on two model 053 multimodality end-fire phantom (CIRS, Norfolk, Virginia) made from Zerdine with six and twelve glass beads embedded. A 3D TRUS scan was acquired from a Philips HDI-3000 and a Terason t3000 for the 6 and 12 bead

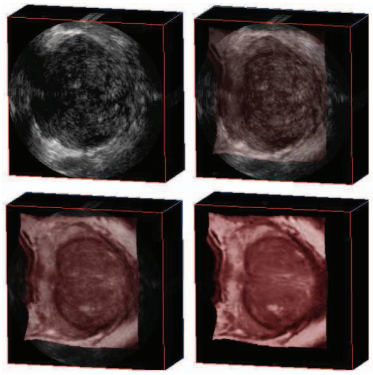

Fig. 3. Visualization of 3D MRI and TRUS blended

Error	Before (mm)	After (mm)
Average Registration (μ)	11.79	3.063
Standard Deviation (σ)	5.9161	1.4134

Table 1. Errors Before and After Registration

phantoms respectively. The six bead phantom was imaged using MRI to acquired high resolution transverse images under different settings: 0.39 mm in-plane (1 mm and 3 mm out-of-plane, 70 cc inflation of Endorectal balloon), 0.54688 mm in-plane (1 mm and 3 mm out-of-plane, No endorectal coil), and 0.54688 mm in-plane (0.7 mm out-of plane with 50 cc inflation). The twelve bead phantom was similarly imaged using the same settings. The fiducial errors computed before and after registration are summarized in Table 1. Figures 4 and 5 show average registration errors for each bead for the 6 and 12 bead phantoms. Bars with slanted lines show original registration error and bars with crisscross lines show final registration errors. The findings of these experiments would need to be corroborated with real patient scans with identifiable markers. An nVidia 8800 GT GPU with 14 multiprocessors running on an Intel Core 2 CPU (6700) at 2.66 GHz was used in this study. The computation time was approximately half a minute (25 seconds for computations and possibly 5-10 seconds for manual initialization of seeds for semiautomatic segmentation).

5. CONCLUSION

In this work, we have demonstrated a prototype system capable of registering two multimodality volumes to perform MRI guided biopsy planning. The two primary goals of this experiment were to achieve small registration errors, and fast registration times. The first goal was found to be satisfactory although extensive validation on more phantoms and real patients would need to be performed. More advanced GPUs introduced recently could further improve computation times (potential speed up of 2 times using the nVidia GTX 280) because of the parallel nature of the algorithms viz surface

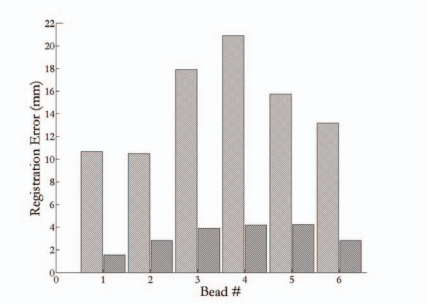

Fig. 4. Mean Registration Errors (μ_{Before}=14.81 mm, μ_{After}=3.26 mm) for 6 Bead Phantom.

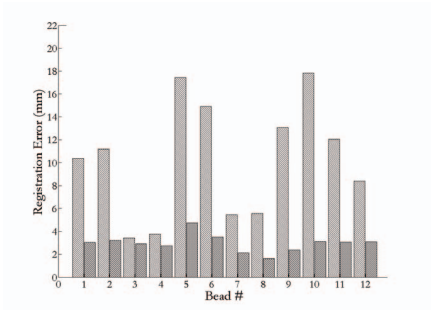

Fig. 5. Mean Registration Errors (μ_{Before}=10.28 mm, μ_{After}=2.96 mm) for 12 Bead Phantom.

registration and elastic interpolation which will scale directly with increasing multiprocessors on the GPU.

6. REFERENCES

[1] A Jemal, R Siegel, E Ward, Y Hao, J Xu, T Murray, and M J Thun, "Cancer statistics 2008," *CA Cancer J Clin*, 2008.

[2] K Shinohara, T M Wheeler, and P T Scardino, "The appearance of prostate cancer on transrectal ultrasonography: correlation of imaging and pathological examinations," *J Urol.*, vol. 142, pp. 76–82, 1989.

[3] J A Jung, F V Coakley, D B Vigneron, M G Swanson, A Qayyum, V Weinberg, K D Jones, P R Carroll, and J Kurhanewicz, "Prostate depiction at endorectal mr spectroscopic imaging: investigation of a standardized evaluation system," *Radiol.*, vol. 233, pp. 701–708, 2004.

[4] P R Caroll, F V Coakley, and J Kurhanewicz, "Magnetic resonance imaging and spectroscopy of prostate cancer," *Reviews in Urology*, vol. 8 (Suppl 1), pp. S4–S10, 2006.

[5] O Akin and Hedvig Hricak, "Imaging of prostate cancer," *Radiol Clin N Am*, vol. 45, pp. 207–222, 2007.

[6] G Fictinger, A Krieger, R C Susil, A Tanacs, L L Whitcomb, and E Atalar, "Transrectal prostate biopsy inside closed MRI scanner with remote actuation under real-time image guidance," *MICCAI*, vol. LNCS 2488, pp. 91–98, 2002.

[7] I Kaplan, N E Oldenburg, P Meskell, M Blake, P Church, and E J Holupka, "Real time MRI-ultrasound image guided stereotactic prostate biopsy," *Magnetic Resonance Imaging*, vol. 20, pp. 295–299, 2002.

[8] C Reynier, J Troccaz, P Fourneret, A Dusserre, C Gay-Jeune, J Descotes, M Bolla, and J Giraud, "MRI/TRUS data fusion for prostate brachytherapy. preliminary results," *Medical Physics*, vol. 31, pp. 1568–1575, 2004.

[9] J Krucker, S Xu, N Glossop, P Guioun, P Choyke, I Ocak, A K Singh, and B J Wood, "Fusion of real-time transrectal ultrasound with preacquired MRI for multi-modality prostate imaging," *SPIE Med. Imag.*, vol. 6509, 2007.

[10] S Xu, J Kruecker, P Guion, N Glossop, Z Neeman, P Choyke, A K Singh, and B J Wood, "Closed-loop control in fused mr-trus image-guided prostate biopsy," *MICCAI*, vol. 4791, pp. 128–135, 2007.

[11] H M Ladak, F Mao, Y Wang, D B Downey, D A Steinman, and A Fenster, "Prostate boundary segmentation from 2d ultrasound images," *EMBS, IEEE Proc 22nd Annual Int. Conf.*, vol. 4, pp. 3188–3191, 2000.

[12] D G Shen, E Herskovits, and C Davatzikos, "An adaptive focus statistical shape model for segmentation and shape modeling of 3D brain structures," *IEEE Trans. Med. Imag.*, vol. 20, pp. 257–271, 2001.

[13] F Shen, R Narayanan, and J S Suri, "Rapid motion compensation for prostate biopsy using gpu," *29th IEEE Annual Int. Conf. , IEEE EMBS*, pp. 3257–3260, 2008.

[14] C Goodall, "Procrustes methods in the statistical analysis of shape," *J. Royal Stat. Soc.*, vol. 53, pp. 285–339, 1991.

[15] C Davatzikos, "Spatial transformation and registration of brain images using elastically deformable models," *CVIU*, vol. 66, no. 2, pp. 207–222, 1997.